N94-15580

OPTIMUM WAVELENGTHS FOR TWO COLOR RANGING

John J. Degnan
Code 901/ Crustal Dynamics Project
NASA Goddard Space Flight Center
Greenbelt, MD 20771

ABSTRACT

The range uncertainties associated with the refractive atmosphere can be mitigated by the technique of two color, or dual wavelength, ranging. The precision of the differential time of flight (DTOF) measurement depends on the atmospheric dispersion between the two wavelengths, the received pulsewidths and photoelectron counts, and on the amount of temporal averaging. In general, the transmitted wavelengths are not independently chosen but instead are generated via nonlinear optics techniques (harmonic crystals, Raman scattering, etc.) which also determine their relative pulsewidths. The mean received photoelectrons at each wavelength are calculated via the familiar radar link equation which contains several wavelength dependent parameters. By collecting the various wavelength dependent terms, one can define a wavelength figure of merit for a two color laser ranging system.

In this paper, we apply the wavelength figure of merit to the case of an extremely clear atmosphere and draw several conclusions regarding the relative merits of fundamental-second harmonic, fundamental-third harmonic, second-third harmonic, and Raman two color systems. We find that, in spite of the larger dispersion between wavelengths, fundamental-third harmonic systems have the lowest figure of merit due to a combination of poor detector performance at the fundamental and poor atmospheric transmission at the third harmonic. Fundamental-second harmonic ($^{\sim}$700 nm and 350 nm) have the highest figure of merit, but second-third harmonic systems, using fundamental transmitters near 1000 nm, are a close second. Raman-shifted transmitters appear to offer no advantage over harmonic systems because of (1) the relatively small wavelength separation that can be achieved in light gases such as hydrogen and (2) the lack of good ultrashort pulse transmitters with an optimum fundamental wavelength near 400 nm.

1 INTRODUCTION

With the subcentimeter precisions available from modern satellite laser ranging (SLR) hardware [Degnan, 1985], atmospheric refraction is a dominant error source in the absolute determination of the geometric range from the station to the satellite. While atmospheric modelling is believed to reduce the systematic errors to roughly one centimeter or less, future progress toward millimeter absolute accuracy ranging will rely on the technique of two color, or dual wavelength, ranging.

In the present paper, we attempt to define optimum wavelengths for two color ranging. In order to accomplish this, we must take into account all of the wavelength dependent parameters which influence our ability to make an accurate differential time of flight (DTOF) measurement. As we will see in the ensuing sections, a proper accounting of wavelength dependent terms will include atmospheric dispersion, atmospheric transmission as a function of sea level visibility, transmit antenna and target gains, detector responsivities, transmitter availability and pulsewidth, and the detailed characteristics of the available non-linear optics techniques for achieving the necessary optical frequency translations.

2 ATMOSPHERIC REFRACTION: THE MARINI-MURRAY MODEL

In the Marini-Murray model of atmospheric refraction [Marini and Murray, 1973], radial variability in the meteorological parameters (i.e. with altitude) is assumed to be governed by the equations for hydrostatic equilibrium, the law of partial pressures, and the perfect gas law. This leads to the following equations for the spherical range correction, SC_{MM}:

$$SC_{MM}(\lambda, E, P_H, T_H, e_H) = \frac{f(\lambda)}{F(\phi, H)} \frac{A(P_H, e_H) + B(\phi, T_H, P_H)}{\sin(E) + \dfrac{B(\phi, T_H, P_H)}{\dfrac{A(P_H, e_H) + B(\phi, T_H, P_H)}{\sin E + .01}}} \tag{2.1}$$

where

$$f(\lambda) = .9650 + \frac{.0164}{\lambda^2} + \frac{.000228}{\lambda^4} \tag{2.2a}$$

$$F(\phi, H) = 1 - .0026 \cos 2\phi - .00031 H \tag{2.2b}$$

$$A(P_H, e_H) = .002357 P_H + .000141 e_H \tag{2.2c}$$

$$B(\phi, T_H, P_H) = 1.084 x 10^{-8} P_H T_H K(\phi, T_H, P_H) + 4.734 x 10^{-8} \frac{P_H^2}{T_H} \frac{2}{3 - \dfrac{1}{K(\phi, T_H, P_H)}} \tag{2.2d}$$

and

$$K(\phi, T_H, P_H) = 1.163 - .00968 \cos 2\phi - .00104 T_H + .00001435 P_H \tag{2.2e}$$

where λ is the laser wavelength in microns, E is the true elevation angle of the satellite in degrees, ϕ is the station latitude, H is the station height above mean sea level, and P_H, T_H and e_H are the surface pressure, temperature, and water vapor pressure at the station. The water vapor pressure e_H is related to the surface percent relative humidity R_H and surface temperature T_H by the equation

$$e_H(R_H,T_H) = \frac{R_H}{100} 6.11 \, x \, 10^{\left(7.5\frac{T_H-273.15}{237.3\cdot(T_H-273.15)}\right)} \qquad (2.3)$$

The wavelength dependence of the range correction is contained in the dispersion term $f(\lambda)$ which is plotted in Figure 1. It was arbitrarily chosen by Marini and Murray to have a value of unity at the ruby laser wavelength of .6943 microns.
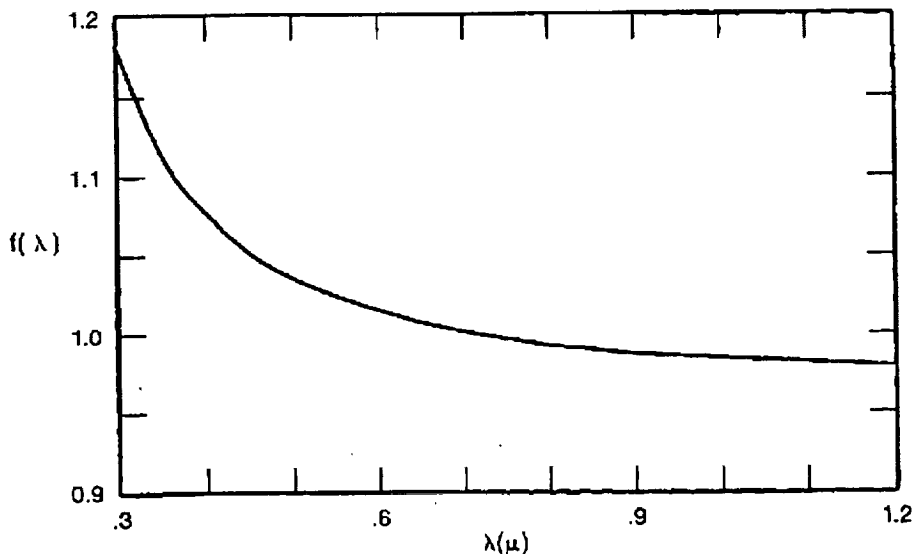

Figure 1. Atmospheric dispersion in a standard atmosphere as a function of wavelength from the near ultraviolet to the near infrared.

3 TWO-COLOR LASER RANGING

By measuring the pulse times-of-flight at two colors and multiplying the results by the velocity of light in vacuum, c, we obtain a measure of the optical path lengths through the atmosphere at the two wavelengths. Thus, the atmospheric refraction correction is given by

$$AC = \gamma(L_1 - L_2) = \frac{\gamma c}{2}(\tau_1 - \tau_2) \tag{3.1}$$

where L_1 and L_2 are the optical path lengths and τ_1 and τ_2 are the measured roundtrip times of flight at the two wavelengths respectively, and

$$\gamma = \frac{n_{g1} - 1}{n_{g2} - n_{g1}} \tag{3.2}$$

where n_{g1} and n_{g2} are the group refractive indices at the two wavelengths. Unfortunately, the wavelength dependence due to the "dry" and "wet" components of the atmosphere are different [Owens, 1968] whereas the expression for the group refractivity N_g used by Marini and Murray assumes no dependence of the water vapor term on wavelength, i.e.

$$N_g(\lambda) = 80.343 f(\lambda)\frac{P}{T} - 11.3\frac{e}{T} \tag{3.3}$$

where P, T, and e are the local pressure, temperature, and water vapor partial pressure respectively. Nevertheless, under normal conditions of modest humidity, γ can be well approximated by the expression [Abshire and Gardner, 1985]

$$\gamma = \frac{f(\lambda_1)}{f(\lambda_2) - f(\lambda_1)} \tag{3.4}$$

where $f(\lambda)$ is given by (2.2a). If we assume that the two times of flight are independently measured, we can express the expected variance in the atmospheric correction as

$$\sigma^2_{AC} = (\gamma c/2)^2(\sigma^2_1 + \sigma^2_2) \tag{3.5}$$

where σ_1 and σ_2 are the RMS errors in the time of flight measurements at the wavelengths λ_1 and λ_2 respectively. In the ideal limit where the differential timing precision is determined only by the signal strength, one can write

$$\sigma_{AC} = \frac{\gamma c}{2}\left(\frac{\tau^2_{p1}}{n_1} + \frac{\tau^2_{p2}}{n_2}\right)^{1/2} \tag{3.6}$$

where τ_{p1} and τ_{p2} are the laser pulsewidths and n_1 and n_2 are the received photoelectron signal strengths at the two wavelengths respectively.

4 THE RADAR LINK EQUATION

The mean signal flux in a range receiver is obtained from the familiar radar link equation. The mean number of photoelectrons n_{pe} recorded by the ranging detector is given by:

$$n_{pe} = \eta_q \left(E_T \frac{\lambda}{hc} \right) \eta_t G_t \sigma \left(\frac{1}{4\pi R^2} \right)^2 A_r \eta_r T_a^2 T_c^2 \qquad (4.1)$$

where η_q is the detector quantum efficiency, E_T is the laser pulse energy, λ is the laser wavelength, h is Planck's constant, c is the velocity of light in vacuum, η_t is the transmit optics efficiency, G_t is the transmitter gain, σ is the satellite optical cross-section, R is the slant range to the target, A_r is the effective area of the telescope receive aperture, η_r is the efficiency of the receive optics, T_a is the one-way atmospheric transmission, T_c is the one way transmissivity of cirrus clouds (when present), and R is the slant range between the station and the target.

In discussing the link equation, we are primarily concerned with those terms which exhibit a wavelength dependence. While optical coatings certainly exhibit a wavelength dependence thereby affecting the transmit and receive optical efficiencies η_t and η_r, coatings can generally be designed to give approximately equal performance once the operating wavelengths are chosen and hence will not be included in our discussion. Similarly, experimental studies of cirrus cloud transmission have shown no significant dependence on wavelength over the band from 0.317 to 12 microns. Other terms in (4.1) do have a wavelength dependence which we will now discuss.

4.1 TRANSMITTER GAIN

A general expression for the transmitter gain is given by

$$G_t = \frac{4\pi A_t}{\lambda^2} g_t(\alpha_t, \beta, \gamma_t, X) \qquad (4.2)$$

where $A_t = \pi a^2$ is the area of the transmitting aperture and $g_t(\alpha_t, \beta, \gamma_t, X)$ is a geometric factor independent of wavelength [Klein and Degnan, 1974]. Note that, for a given transmit aperture and a well-collimated system, the transmitter gain is inversely proportional to the wavelength squared.

4.2 TARGET OPTICAL CROSS-SECTION

The optical cross-section of an unspoiled retroreflector is given by [Degnan, 1992]

$$\sigma_{cc} = \rho A_{cc} \left(\frac{4\pi A_{cc}}{\lambda^2} \right) \qquad (4.3)$$

where ρ is the cube corner reflectivity, $A_{cc} = \pi R_{cc}^2$ is the light collecting area of the corner cube, and $4\pi A_{cc}/\lambda^2$ is the on-axis retroreflector gain. Even in the presence of complicating factors such as velocity aberration and retroreflector

spoiling, an array of retroreflectors designed to operate at
both wavelengths would be expected to retain the same inverse
square law dependence on wavelength exhibited by (4.3).

4.3 ATMOSPHERIC ATTENUATION

In the near-ultraviolet to visible spectral band between 0.3
and 0.7 μ, atmospheric attenuation is dominated by aerosol
(Mie) scattering but molecular (Rayleigh) and ozone absorption
also play a role [RCA, 1968]. In the near infrared beyond
0.7μ, the plot of atmospheric transmission versus wavelength
(see Figure 2) is modulated by strong absorption features of
various molecular constituents in the atmosphere, notably
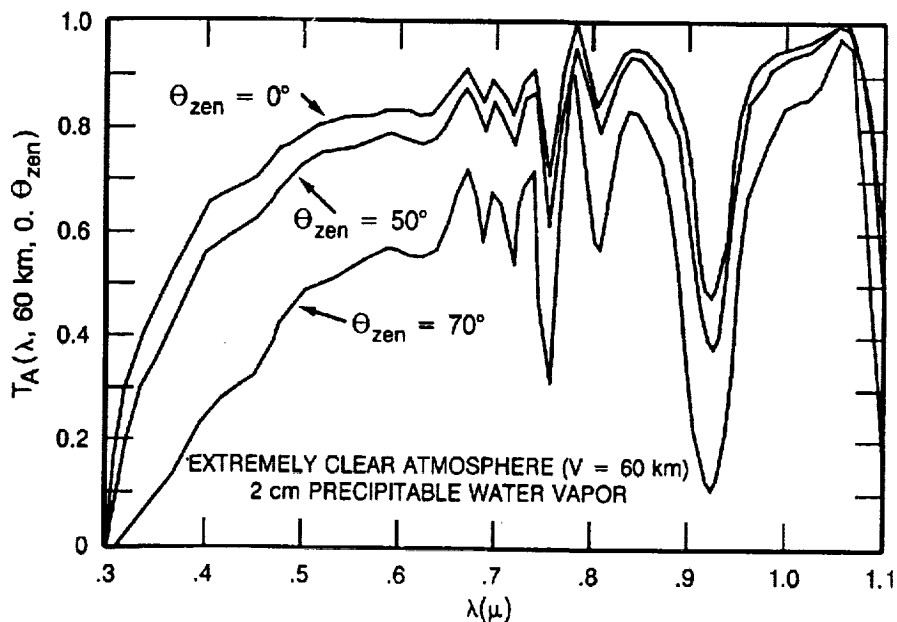water vapor, oxygen, and carbon dioxide.

Figure 2. Atmospheric transmission as a function of wavelength
under extremely clear conditions with 2 cm of precipitable
water vapor at zenith angles of 0, 50, and 70° (corresponding
to 1, 2, and 3 air masses) respectively.

The transmission curve presented in Figure 2 corresponds to
excellent "seeing" conditions (80 Km visibility) and 2 cm of
precipitable water vapor. It should be noted that atmospheric
seeing conditions vary widely from day to day and from site to
site and are usually characterized by "sea level visibility"
expressed in kilometers. Plots of the sea level attenuation
coefficient versus wavelength (from 0.4 to 4 μ) as a function
of sea level visibility can be found in the RCA Electro-Optics

Handbook [RCA,1968]. For the purpose of this analysis, how-
ever, we will consider only the extremely clear atmosphere
depicted in Figure 2.

4.4 OPTICAL DETECTORS

Finally, the availability of high quantum efficiency optical
detectors at the two laser wavelengths is important. If a com-
mon photocathode is to be used, such as in most streak camera
schemes for performing differential timing, the photocathode
must be sensitive at both wavelengths. However, since the
images of the two return pulses can be spatially separated in
the entrance slit of the streak camera, one can conceive of
specially constructed streak tubes containing more than one
photocathode material to obtain the highest sensitivity at
both wavelengths. It may also be possible, at some future
date, to do the necessary timing via electronic means, such as
high speed GaAs technology, without resorting to streak camera
technology although this capability has not yet been demon-
strated.

A) "BEST" PHOTOEMISSIVE DETECTOR RESPONSIVITIES

WAVELENGTH (μ)	RESPONSIVITY	PHOTOCATHODE (+ WINDOW) MATERIAL
.3	50	S20
.35	60	K-Cs-Sb – (LIME GLASS)
.40	80	K-Cs-Sb – (LIME GLASS)
.45	70	K-Cs-Sb – (LIME GLASS)
.50	63	K-Cs-Sb + (LIME GLASS)
.55	64	GaAs (+ 9741 GLASS)
.60	65	GaAs (+ 9741 GLASS)
.65	67	GaAs (+ 9741 GLASS)
.70	68	GaAs (+ 9741 GLASS)
.75	69	GaAs (+ 9741 GLASS)
.80	70	GaAs (+ 9741 GLASS)
.85	68	GaAs (+ 9741 GLASS)
.90	13	GaAs (+ 9741 GLASS)
.98	9	GaInAs (+ 9741 GLASS)
1.02	.8	GaInAs (+ 9741 GLASS)
1.1	.2	S1

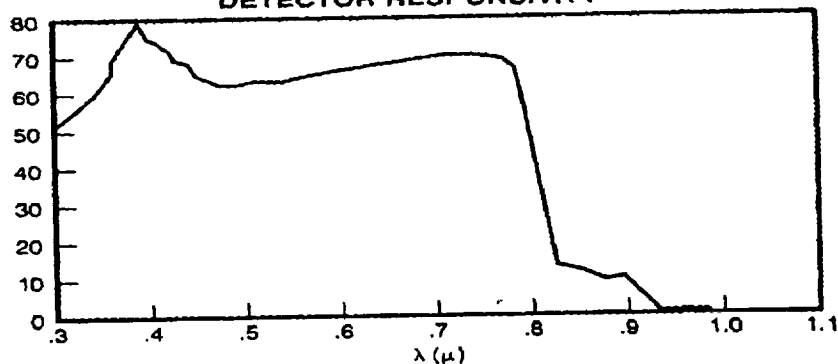### B) COMPOSITE GRAPH OF PHOTOEMISSIVE DETECTOR RESPONSIVITY

Figure 3. Summary of "best" photoemissive detector responsivi-
ties from the near ultraviolet to the near infrared.

Detector sensitivity at a particular wavelength is usually expressed as "spectral responsivity" in milliamperes/Watt. It is related to quantum efficiency by the equation

$$\eta_q(\lambda) = R(\lambda)\frac{hc}{\lambda e}$$

(4.4)

where $R(\lambda)$ is the detector spectral responsivity at wavelength λ, h is Planck's constant, and c is the velocity of light. A composite responsivity curve, which is the envelope of individual responsivity curves for some common visible and near infrared photoemissive detectors[Slater, 1980; Zwicker, 1977] is illustrated in Figure 3.

5 "OPTIMUM" WAVELENGTHS FOR TWO COLOR SLR

In choosing "optimum" candidate wavelengths for successful two color ranging, there are a variety of technical issues the engineer must consider. These will be discussed in the ensuing subsections. As we shall now see, equation (3.6) for the RMS error in the atmospheric correction for the photon-limited case, combined with the radar link equation (4.1), points the way to the selection of a set of optimum wavelengths. Since we want to minimize σ_{AC}, the inverse of (3.6) can serve as an overall system figure of merit.

5.1 ATMOSPHERE

The dependence of (3.6) on the atmospheric dispersive function $f(\lambda)$ illustrates the need for adequate atmospheric dispersion between the two wavelengths in order to reduce the severity of the timing requirements. The atmospheric dispersion curve in Figure 1 strongly suggests that one wavelength be chosen to lie in the near ultraviolet. On the other hand, atmospheric attenuation in the spectral band between 0.3 and 0.7 microns, resulting from the combined effects of molecular (Rayleigh) and aerosol (Mie) scattering and ozone absorption, also increases rapidly in the near ultraviolet as shown in Figure 2. This will negatively impact the timing precision by lowering the photoelectron count at the UV wavelength. Furthermore, in choosing a laser wavelength, it is probably wise to avoid the strong water absorption lines in the spectral regions between 0.7 and 1.0 microns and beyond 1.1 micron. The high variability of water vapor total burden would impact both the day-to-day signal strength and cause the pulse group velocity to vary via the anomalous dispersion effect near an absorbing feature.

5.2 LASER TRANSMITTER

The availability of lasers capable of generating high peak powers and ultrashort pulsewidths on the order of 35 picoseconds or less is also a consideration. Preference is generally given to solid state lasers because of the practical difficulties of using liquid dye lasers in the field. Over the

past decade, much progress has been made in the development of highly tunable solid state lasers such as Alexandrite (700 to 810 nm) and Titanium-doped sapphire (600 to 900 nm). The wide bandwidths of these new materials are capable of supporting subpicosecond pulsewidths whereas today's workhorse, Nd:YAG, is limited to about 10 picoseconds by it's relatively narrow linewidth (120 GHz). However, high bandwidth comes at a price - i.e. lower gain - making the construction of high peak power Ti:Sapphire and Alexandrite devices more difficult.

Generally, the wavelengths in two color systems are generated from the fundamental wavelength λ_f via nonlinear optical techniques such as harmonic generation in crystals or Raman shifting in gases. This assures simultaneity of emission and eliminates (thankfully) the need to synchronize the firings of two separate lasers with picosecond precisions. However, reliance on nonlinear teqhniques implies that the two wavelengths cannot be chosen independently of each other. In the case of harmonic generation, the second and third harmonic wavelengths are given by

$$\lambda_2 = \frac{\lambda_1}{2} \qquad\qquad \lambda_3 = \frac{\lambda_1}{3} \qquad\qquad (5.1)$$

respectively.

In Raman shifting, a portion of the incident radiation at input frequency, ν_o is shifted by some fixed amount ν_s (the "Stokes shift") toward longer wavelengths relative to the fundamental. One also obtains frequencies at longer ("Stokes") and shorter ("Anti-Stokes") wavelengths, but these are generally too weak to supply sufficient energy for satellite ranging. Large Stokes frequency shifts, and hence high dispersion between wavelengths, are obtained by Raman shifting in light gases. Hydrogen produces the largest shift of 4155 cm^{-1}, and photon conversion efficiencies as high as 80% have been reported. For example, one proposed two color SLR system uses the second harmonic of Nd:YAG (532 nm) in hydrogen to obtain a second wavelength output at 680 nm [Gaignebet et al, 1986].

A second consequence of harmonic or Raman generation is that the pulsewidth of the secondary wavelength is generally shorter than the pulsewidth of the fundamental. From the theory of harmonic generation [Degnan, 1979], the harmonic pulsewidths are approximately given by

$$\tau_{2h} \sim \frac{\tau_1}{\sqrt{2}} \qquad\qquad \tau_{3h} \sim \frac{\tau_1}{\sqrt{3}} \qquad\qquad (5.2)$$

for low to moderate energy conversion efficiencies (< 50% - the usual case). Raman generation depends on third order nonlinear processes, and the pulsewidth dependence is identical to that of third harmonic generation.

5.3 WAVELENGTH FIGURE OF MERIT

In order to treat all potential system configurations on an equal basis, some assumptions are in order. We will assume that the fundamental laser, from which all other wavelengths are derived, is characterized by an energy E and a pulsewidth τ_p which is constant for all wavelengths. Thus, Equation (3.6) becomes

$$\sigma_{AC} = \gamma c \tau_p \sqrt{\frac{1}{\beta_1^2 n_1} + \frac{1}{\beta_2^2 n_2}} \qquad (5.3)$$

where β_1 and β_2 are pulsewidth scale factors which depend on the nonlinear process used to generate them as in (5.2). In addition, we recognize that wavelengths derived via nonlinear processes are obtained with some typical energy efficiency which we will denote by η_1 and η_2 respectively. If the fundamental wavelength is used as one of the two wavelengths, we will assign values of $\beta_f = 1$ and $\eta_f = 1$. For second and third harmonic generation in the ultrashort pulse regime, typical conversion efficiencies are $\eta_{sh} = .5$ and $\eta_{th} = .2$ respectively.

In order to derive a wavelength figure of merit, we must now bring together all of the wavelength dependent terms in equations (4.1) and (3.5). We obtain for the figure of merit

$$F(\lambda_1, \lambda_2, E) = \frac{f(\lambda_1) - f(\lambda_2)}{f(\lambda_1)} \left[\frac{\lambda_1^4}{\eta_1 \beta_1^2 R(\lambda_1) T_a^2(\lambda_1, E)} + \frac{\lambda_2^4}{\eta_2 \beta_2^2 R(\lambda_2) T_a^2(\lambda_2, E)} \right]^{-\frac{1}{2}}$$

$$(5.4)$$

where $f(\lambda)$ is the wavelength dispersion term in the Marini-Murray atmospheric correction formula, η_1 and η_2 and β_1 and β_2 are the energy conversion efficiencies and pulsewidth reduction factors respectively for the relevant nonlinear process, $R(\lambda)$ is the spectral responsivity, and $T_a(\lambda, E)$ is the one way atmospheric transmission as a function of wavelength and elevation angle. The factor of λ^4 comes from the combined inverse square law dependence of the transmitter and target (retroreflector) gains on wavelength. The additional factor of λ associated with converting detector quantum efficiency to spectral responsivity cancels with a similar factor in (4.1) which converts transmitter laser energy to the number of transmitter photons. In plotting (5.4), we will use the envelope of the individual photoemitter responsivity curves in Figure 3 so that we present each wavelength in its most favorable light.

6 CONCLUSIONS

Figure 4 provides plots of the wavelength figure of merit as a function of the fundamental (laser) wavelength and elevation angle for the extremely clear atmosphere depicted in Figure 2. Parts (a), (b), and (c) correspond to elevation angles of 90, 45, and 20 degrees respectively. The three curves within each plot compare systems which use: (1) the fundamental and second harmonic wavelengths; (2) the fundamental and third harmonic wavelengths; and (3) the second and third harmonic wavelengths.

In spite of their greater dispersion, fundamental-third harmonic systems have the lowest figure of merit at all elevation angles due to a combination of poor detector performance at the fundamental and poor atmospheric transmission at the third harmonic. The performance of these systems peaks at a fundamental wavelength of about .97 microns independent of elevation angle.

At zenith, fundamental-second harmonic systems, operating at wavelengths of 670 and 335 nm, have the highest figure of merit ($F = 1.75$) but second-third harmonic systems, operating at wavelengths of 525 and 350 nm (fundamental = 1050 nm), are almost as good ($F = 1.6$). As one progresses to smaller elevation angles, atmospheric attenuation in the ultraviolet begins to dominate and the optimum fundamental wavelength is shifted toward longer wavelengths with a corresponding reduction in the wavelength figure of merit. Thus, the Nd:YAG laser, with a fundamental wavelength of 1064 nm and a very mature technology, is a near-optimum choice for a second-third harmonic system. However, a fundamental-second harmonic system which utilizes a Ti:Sapphire laser operating in the near infrared beyond 670 nm is a possible alternative.

Figure 5 suggests that a fundamental wavelength of about 400 nm is optimum for a hydrogen Raman-shifted laser and that these systems offer no real advantage over harmonic systems because of their lower wavelength figure of merit. This conclusion is further supported by the fact that there are no high power solid state lasers operating in the near ultraviolet. The principle short wavelength devices are excimer ("excited dimer") gas discharge lasers. At present, excimers cannot achieve ultrashort pulsewidths on the order of picoseconds, typically operate in the high atmospheric attenuation region of the spectrum below 360 nm, and are operationally less desirable than high power solid state lasers. Doubling or tripling solid state lasers to achieve a near ultraviolet wavelength prior to Raman shifting only decreases the overall wavelength figure of merit further by reducing the values for the energy efficiency factors η_1 and η_2. However, this effect is partially offset by the slight reduction in pulsewidth (increased β values) resulting from nonlinear generation.
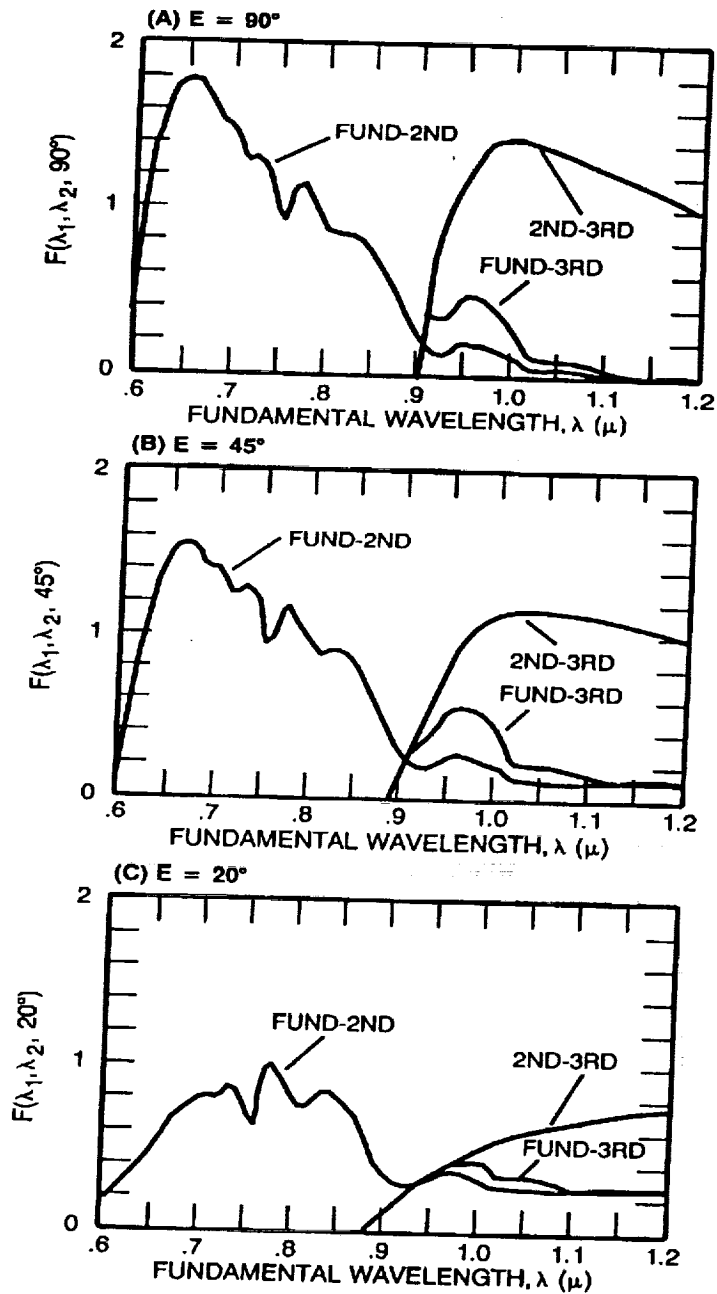
Figure 4. Two color wavelength figure of merit for fundamental-second harmonic, fundamental-third harmonic, and second-third harmonic systems operating in an extremely clear atmosphere at elevation angles of (a) 90°, (b) 45° and (c) 20° respectively.
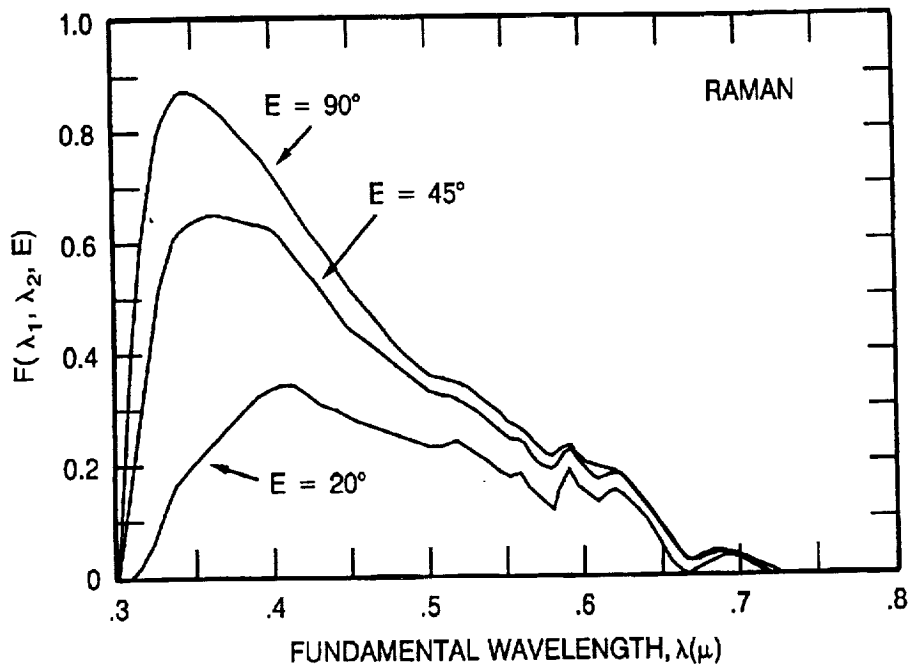
Figure 5. Two color wavelength figure of merit for Raman systems operating in an extremely clear atmosphere at elevation angles of 90°, 45° and 20°.

7 REFERENCES

Abshire, J. B. and C.S. Gardner, "Atmospheric refractivity corrections in satellite laser ranging", IEEE Trans. on Geoscience and Remote Sensing, GE-23, pp. 414-425, 1985.

Degnan, J. J., "Physical processes affecting the performance of high-power, frequency-doubled short pulse laser systems: analysis, simulation, and experiment", Ph.D. Dissertation, University of Maryland, College Park, MD, May 1979.

Degnan, J. J., "Satellite Laser Ranging: Current Status and Future Prospects", IEEE Trans. on Geoscience and Remote Sensing, GE-23, pp. 398-413, 1985.

Degnan, J. J., "Millimeter Accuracy Satellites for Two Color Ranging", these proceedings (1992).

Gaignebet, J., F. Baumont, J. L. Hatat, K. Hamal, H. Jelinkova, and I. Prochazka, "Two wavelength ranging on ground target using Nd:YAG 2HG and Raman 0.68 μm pulses", Proceedings of the Sixth International Workshop on Laser Ranging Instrumentation, Antibes-Juan Les Pins, France, September 22-26, 1986.

Klein B. J., and J. J. Degnan, "Optical antenna gain. 1. Transmitting antennas", Applied Optics, 13, pp. 2134-2140, 1974.

Marini, J. W. and C. W. Murray, "Correction of laser range tracking data for atmospheric refraction at elevations above 10 degrees", NASA Report X-591-73-351, Goddard Space Flight Center, 1973.

Owens, J. C., "Optical refractive index of air: Dependence on pressure, temperature, and composition", Applied Optics, 6,51-58, 1967.

RCA Electro-optics Handbook, Technical Series EOH-10, RCA Commercial Engineering, Harrison, NJ, 1968.

Slater, P. N., Remote Sensing: Optics and Optical Systems, Chapter 13, Addison-Wesley Publishing Co., Reading, Massachusetts, 1980.

Zwicker, H. R., "Photoemissive Detectors", in Optical and Infrared Detectors, Ed. R. J. Keyes, Springer Verlag, New York, 1977.